Linear Viscoelastic Behavior of End-Tethered Polymer Monolayers at the Air/Water Interface

Clarisse Luap* and Werner A. Goedel†

Max-Planck-Institut für Kolloid-und Grenzflächenforschung, Berlin, Germany

Received August 31, 1999; Revised Manuscript Received June 30, 2000

ABSTRACT: We investigate the rheological behavior of Langmuir monolayers consisting of polyisoprene chains tethered by one end to the air/water interface. These 10−50 nm thick monolayers provide model systems of a molten polymer brush for which the ends can move within the interface. Their linear viscoelastic properties are determined by applying a small-amplitude shear flow within the interface plane and investigated as a function of surface density and length of tethered chains. When increasing the chain length, we observe a transition from a liquidlike to a transient network behavior typical of entangled bulk polymer melts. The terminal relaxation time and the effective bulk zero shear viscosity of the monolayers are 2−3 orders of magnitude higher than those of a linear bulk polyisoprene melt of identical molecular weight. Both quantities are shown to exhibit an enhanced molecular weight dependence and to increase with surface density.

1. Introduction

When polymer chains are tethered by one end to a flat and impenetrable surface, with lateral spacings small compared to the unperturbed dimensions of the polymer coils, chains will stretch away from the interface and form a so-called polymer brush.[1] These layers have attracted considerable attention due to the importance of end-tethered chains for the improvement of surface properties in various areas, such as adhesion, lubrication, and the design of biocompatible materials.[2] Beyond these practical interests, the polymer brush allows to address several important problems of fundamental polymer science: It is the simplest case of a thin polymer film at the vicinity of a surface for which both the reduced dimensionality and the influence of the surface are expected to lead to peculiar properties. It serves as a basis to understand complex bulk systems with similar features of end confinement and chain anisotropy, like phase-separated and interface-restricted block copolymers or polymeric micelles. In this context, it is of relevance to determine how properties in a layer of end-tethered chains differ from the bulk case. Among various properties, the chain dynamics remain by far less understood than that of free chains in the melt or solution. In the bulk, it is established that dynamical properties exhibit universal scaling behavior with the chain length.[3] A major characteristic is the existence of a critical chain length above which the dynamics are controlled by topological constraints, e.g., entanglements, that restrict individual chain motions. For a layer of end-tethered chains questions which naturally arise are the following: (i) How are the dynamics of chains affected by their anisotropy and end confinement? (ii) Does the stretching of chains influence the development of topological constraints and delay the crossover to entanglement-dominated motions?

Part of these issues have been addressed in experimental studies on block copolymers in the lamellar phase. Dielectric spectroscopy studies[4] showed that the lamellar ordering induces a broadening and a retardation of relaxation processes. Importantly, Lodge et al.[5,6] emphasize the role of entanglements in retarding the lateral diffusion of block copolymer chains parallel to the interface between microdomains. However, in these bulk systems, chain entanglement can occur in the interpenetration zone of adjacent layers. It remains thus unclear whether entanglements can occur by lateral overlapping of chains within individual layers.

Yet, few studies considered fundamental aspects of chain dynamics for the single brush layer case. Most theoretical treatments[8,9] and computer simulation studies[10−12] were restricted so far to the short chain regime. Experimentally, tethering of polymer chains can be achieved via covalent bonding or physical adsorption of an ionic end group or of a short second polymer block. In most studies this bonding was achieved via exposing a solid interface to a solution of suitable polymers, and grafted swollen polymer brushes were obtained. Some insights into the chain dynamics of these swollen brushes were obtained by dynamic light scattering.[7] Another approach particularly suitable to evidence entanglement constraints is to analyze the response of a polymer brush to a flow field and determine its rheological properties. Up to now, rheological studies treated grafted swollen brushes, imposing a transverse shear flow within a surface force apparatus (SFA). Particular attention has been given to the influence of end-tethered layers on adhesion and friction forces (see ref 13 and references herein). Using the SFA to apply a small-amplitude oscillatory tranverse shear flow, the linear viscolasctic properties of molecularly thin polymer layers[14] as well as polymer brushes[15] could be investigated. With this method, Pelletier et al.[16] observed a finite shear modulus in a highly compressed brush/mica system in good solvent, suggesting the presence of chain entanglements in a single brush layer.

In this contribution, we report for the first time on the rheological properties of molten polymer brushes as Langmuir monolayers at the air/water interface (see Figure 1). The monolayers consist of hydrophobic poly-

* Corresponding author. E-mail: clarisse.luap@gmx.net.
† Present address: Organic Chemistry 3, University of Ulm, Albert-Einstein-Allee 11, D-89069 Ulm, Germany.

10.1021/ma991485i CCC: $20.00
Published on Web 02/03/2001

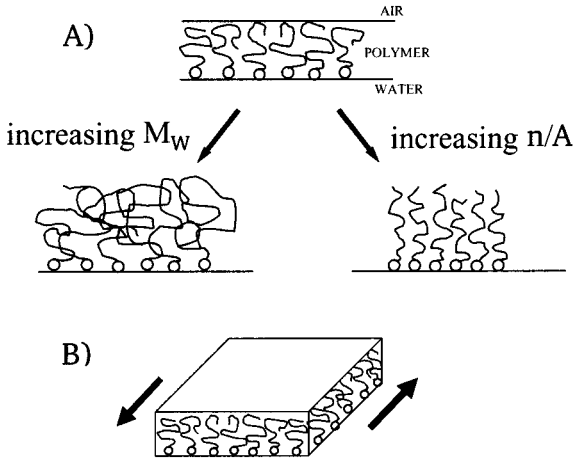

Figure 1. (A) Schematic diagram of an annealed melt polymer brush as Langmuir monolayer of end-tethered polymers at the air/water interface. The brush keeps a constant density; therefore, its height can be controlled by varying either the molecular weight M_w or the tethering density n/A. The amount of entanglement-like topological constraints and degree of anisotropy tend to increase with M_w and n/A, respectively. (B) Effects of both parameters on chain dynamics are probed by applying a small-amplitude oscillatory shear flow within the interface plane (in-plane shear).

mer chains terminated with an ionic headgroup and provide model systems of a molten polymer brush for which the ends can move within the interface (usually referred to as an annealed molten polymer brush).[18] These monolayers offer a unique opportunity to explore basic properties of end-tethered chains in detail. As illustrated in Figure 1A, the monolayer thickness can be varied either by changing the molecular weight or by changing the surface density of tethered chains. Since the polymer brush is solvent-free, these are the only parameters determining chain dynamics. Both can be varied in a well-defined way and independently. The surface (or tethering) density, given by the inverse of the mean area per molecule A/n, is directly obtained from the amount of polymer and the covered water surface area. In between rupture and collapse of the polymer monolayers, the surface density of the monolayers investigated here can be varied by a factor of 2 via lateral compression or expansion with the barrier of a Langmuir trough. In addition, one can easily determine the lateral pressure[17] and thus characterize the thermodynamic state of the system, especially rupture of the monolayer at zero surface pressure and collapse at high surface pressure.

Here, the linear viscoelastic properties of the monolayer are determined in situ by applying a small-amplitude oscillatory shear flow within the interface plane (Figure 1B). Since the chain ends are free to move within the interface plane, this method known as surface (or two-dimensional) shear rheology is particularly suitable to identify topological constraints. For this purpose, and in order to identify relaxation processes, like in conventional rheology of bulk polymer melts, the response of the monolayers is probed within a wide range of frequencies. The frequency-dependent shear dynamic moduli as well as the zero shear viscosity are presented for molecular weights comparable to and larger than the critical molecular weight for entanglement of the bulk polymer. Systematic variation of the tethering density and comparison with the corresponding bulk properties allow us to characterize effects of end confinement, anisotropy, and reduced dimensionality on the dynamical properties of polymer melts.

Table 1. Characteristics of the Polymers Used: Number-Average Molecular Weight M_n, Polydispersity Index I, and Average Number of Repeat Units N

name	M_n [g/mol]	I	N
PI-10K	9 638	1.14	142
PI-20K	20 820	1.04	306
PI-36K	36 540	1.02	537
PI-46K	45 900	1.02	675
PI-55K	55 020	1.02	809

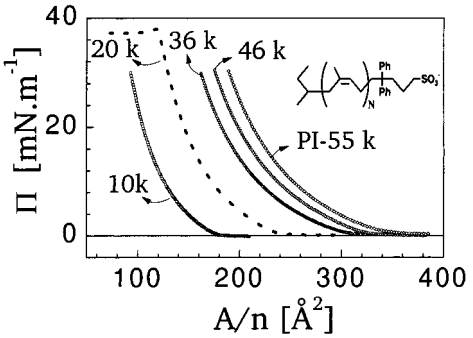

Figure 2. Isotherms—lateral pressure Π vs the mean area per molecule A/n—of the sulfonated polyisoprenes taken from ref 18. The different molecular weights are indicated using the notations of Table 1. For the PI-20K sample, the isotherm is represented down to the collapse region. The collapse pressure is about 37 mN/m and identical for all molecular weights.

2. Experimental Section

Melt Polymer Brush as Monolayers at the Air/Water Interface. The brushlike monolayers used in this study have been presented in detail in ref 18. The systems consist of a set of linear polyisoprene chains of molecular weights ranging from 10 to 55 kg/mol, terminated by a sulfonated (SO_3^-) headgroup. The polyisoprene chains contain about 71% *cis*-1,4, 22% *trans*-1,4, and 7% 3,4 units. The critical molecular weight for entanglement onset $M_{c,bulk}$ of bulk polyisoprenes with similar microstructures is around 10−15 kg/mol,[19,20] so that the molecular weights studied here cover approximately a range between 1 and $5M_{c,bulk}$. The polymers will be called PI-*X*K where *X* is the approximate molecular weight in kg/mol; see Table 1 for details.

Monolayers at the air/water interface are obtained by spreading a dilute solution ($c < 5 \times 10^{-5}$ mol/L) of the polymer onto the water surface of a Langmuir trough at room temperature. Chloroform (Aldrich, 99.9% pure) is used as a spreading solvent. Water (resistivity 18.2 MΩ/cm) was purified with an ion exchange/filter system (Millipore). After evaporation of the solvent, lateral compression and/or expansion of the monolayer with the Teflon barrier of a Langmuir trough leads to reversible and hysteresis-free lateral pressure−area isotherms. Isotherms corresponding to the different molecular weights are shown in Figure 2. It has been previously demonstrated that at large areas per molecule (zero lateral pressure) there is a coexistence between patches of monolayer and bare water surface. As soon as the pressure exceeds zero, a continuous and laterally homogeneous film is formed which, when the pressure exceeds 37 mN/m, collapses into droplets. In between these lateral pressures, the homogeneous monolayer keeps a constant 3-dimensional density equal to the density of the bulk material.[18,21] Hence, the film thickness h varies with the tethering density n/A according to $h = N\nu(n/A)$, where N is the number of repeat units per chain and $\nu = 123.7$ Å^3, the volume of a repeat unit calculated from the bulk density of polyisoprene.[18,21]

Interfacial Rheology. The setup for the rheological experiments is based on a commercial interfacial rheometer

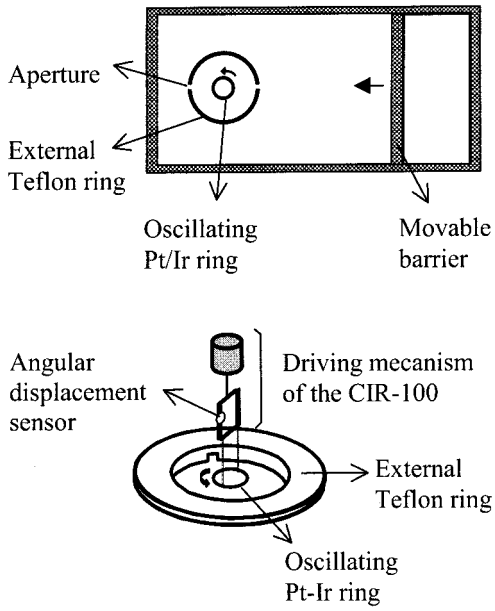

Figure 3. Schematic drawing of the experimental setup: the top part shows a horizontal cut view of the Langmuir trough in the air/water interface plane; the lower part shows in more detail the measuring area.

(CIR-100 from Camtel Ldt., Royston, UK) which has been equipped with a rectangular Langmuir trough (Riegler & Kirstein, Wiesbaden, Germany). Measurements are performed in a two-concentric-ring geometry in order to produce a two-dimensional Couette flow within the interface (see Figure 3). The inner ring (a Pt/Ir De Nouy ring of diameter 13 mm) is driven to perform small-amplitude oscillatory rotational motion. Following the method of ref 22, the external ring is in Teflon (diameter 46 mm) and mounted on the trough such that it can touch the interface and limit the measuring area of the monolayer. This external ring has two small apertures (5 mm each) to allow equilibration of the lateral pressure between both parts of the monolayer. The trough is equipped with one Teflon barrier for lateral compression. Two Wilhelmy plate devices monitor independently the lateral pressure outside and inside the measuring area.

The rheometer[23] operates in a force oscillation mode between 10^{-3} and 20 Hz. A sinusoidal torque is applied, and the corresponding angular displacement is recorded. Below 2 Hz, the natural frequency of the instrument, the surface storage $G'_s(\nu)$ and loss $G''_s(\nu)$ moduli are obtained from the amplitude ratio and phase lag between torque and displacement (the conventional method used by stress controlled rheometer[24]). Above 2 Hz, $G'_s(\nu)$ and loss $G''_s(\nu)$ are determined according to the method of normalized resonance,[23,25] which uses a feedback network to restore the resonance condition at a given frequency and amplitude of angular displacement.

Before measuring the properties of the film-covered surface, the response of the pure water surface is recorded as a reference. Moduli of the monolayers are extracted by subtracting the response recorded for the pure water surface from the response of the film-covered surface.[26] This procedure assumes that the torques transmitted to the film and to the subphase are additive and decoupled.

Experimental Procedure and Errors. All rheological measurements were performed at 20 °C, under an inert atmosphere (Ar or N_2), to avoid degradation of the polyisoprene chains. The strain amplitude was in all cases lower than 5%.

If the inner and outer rings are brought into contact with the water surface and the polymer is spread outside the measuring area, only the low molecular weight compounds (M_n < 36 kg/mol) flow easily through the openings of the outer ring. In the case of the longer polymers, significant pressure differences inside and outside the measuring area are observed during the compression/expansion of the monolayer. Therefore, two different procedures are used.

For the lowest molecular weight compounds (M_n < 36 kg/mol), spreading is performed outside the measuring area directly after the reference measurement with inner and external rings prepositioned at the interface. The viscoelastic properties of the film are determined at different points (Π, A/n) of the isotherm by stepwise compression/expansion of the monolayer.

For the higher molecular weight compounds, a homogeneous film is prepared at the required (Π, A/n) on the free water surface of the rectangular trough. The external and inner rings are brought into contact with the monolayer afterward. Equilibration of the lateral pressure is checked with the two Wilhelmy plate devices before conducting the rheological measurements.

With the intermediate molecular weight (PI-20K), we could verify that both methods lead to identical results within the experimental error. Experimental errors are estimated from the dispersion of the data obtained on different samples measured under the same conditions. These are typically of 10% and 20% for the low and high molecular weight compounds, respectively.

3. Results

Results are presented from two different viewpoints. In the first part, no assumptions on the inner structure of the monolayer are made. The monolayer is regarded as a strictly 2-dimensional (2D) object, and data are presented as surface or 2D viscoelastic properties.

In the second part, we take into account that the monolayer has a finite thickness (10−50 nm) which is proportional to the tethering density and the length of the polymer chain. The 2D moduli are converted to 3-dimensional (3D) moduli by dividing by the thickness of the monolayer. Assuming that the shear stress and strain are transmitted homogeneously through the overall film thickness, these effective 3D moduli correspond to the actual bulk moduli of the monolayer. They can be directly compared to 3D moduli of bulk systems and thus can be used to quantify the effects of end confinement and reduced dimensionality on chain dynamics.

3.1. Two-Dimensional Viscoelastic Properties. 3.1.1. Effect of Molecular Weight. We first describe the qualitative viscoelastic behavior of the monolayers revealed by the frequency dependencies of the surface storage and loss moduli. Figure 4A−C represents, in double-logarithmic scales, the 2D dynamic moduli vs frequency, at a constant lateral pressure $\Pi = 10$ mN/m, for three different molecular weights.

The lowest molecular weight compound PI-10K (Figure 4A) exhibits a viscous response within the entire frequency range. The storage modulus values remain below the resolution of the instrument (which is approximately 0.1 mN/m). The loss modulus follows approximately the power law expected for a liquid of constant viscosity η: $G'' = \eta\omega$.

The monolayers of high molecular weights (PI-36K and higher, see Figure 4B,C) show the qualitative features of a transient network behavior typical of entangled polymer melts.[24,27] One can distinguish a frequency region where the storage modulus exceeds the loss modulus and hence where the monolayer responds predominantly with a rubberlike character. At low frequencies, a liquidlike response is recovered ($G'' > G'$), and the moduli reach the characteristic limiting behavior $G'(\omega) \propto \omega^2$ and $G'' \propto \omega$. Like for entangled polymer melts, we will refer to these two distinct regions as the "rubbery plateau" (or plateau region) and "terminal

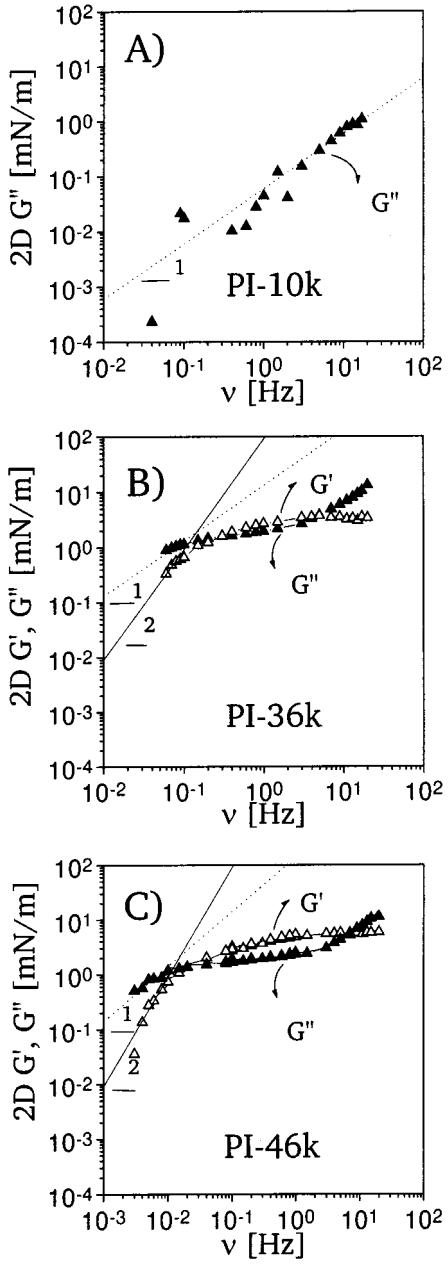

Figure 4. Evolution of the linear viscoelastic behavior with molecular weight at a lateral pressure $\Pi = 10$ mN/m: 2D storage modulus (△) and loss modulus (▲) vs frequency on double-logarithmic scales. (A) Sample PI-10K. (B) Sample PI-36K. (C) Sample PI-46K. Lines (—, · · ·) represent the limiting behaviors $G'(\omega) \propto \omega^2$ and $G'' \propto \omega$, respectively.

zone", respectively. At a fixed frequency of around 5 Hz appears another regime where G'' crosses and then dominates G'. For bulk polymer melts, such crossing marks the onset of the rubber-to-glass transition.[24] Our experiments are performed at more than 80 °C above the glass transition of polyisoprene. A rubber-to-glass transition is thus quite unexpected in this frequency range. Since this regime occurs when the mechanical response starts to be dominated by inertia effects, we will not discuss it further and concentrate on responses at longer time scales.

The shape of the dynamic moduli reflects a very smooth transition from a predominantly rubberlike to liquidlike behavior. The rubber character becomes more pronounced and extends to lower frequencies with increasing molecular weight.

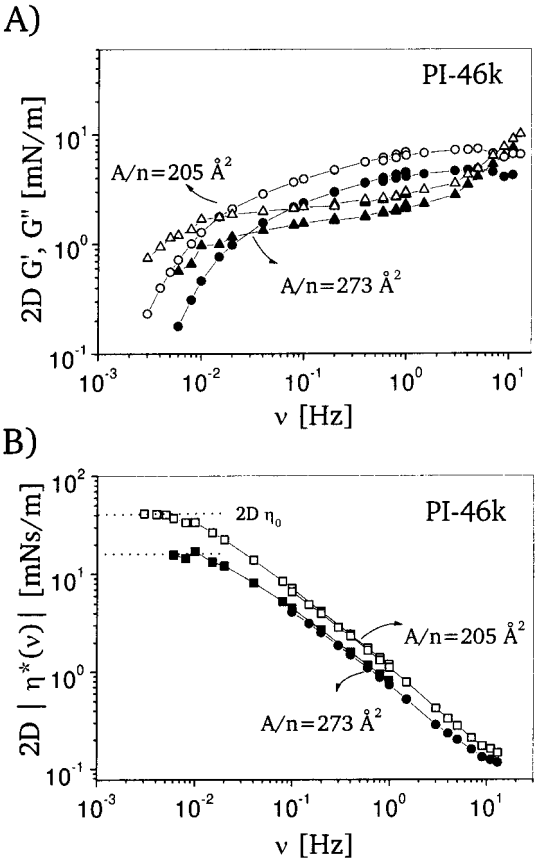

Figure 5. Effect of surface density on the viscoelastic behavior: Sample PI-46K at $A/n = 205$ Å^2, $\Pi = 20$ mN/m (open symbols) and $A/n = 273$ Å^2, $\Pi = 5$ mN/m (filled symbols). (A) 2D storage modulus (circles) and loss modulus (triangle) vs frequency on double-logarithmic scales. (B) Modulus of the 2D complex viscosity vs frequency on double-logarithmic scales.

The frequency marking the onset of terminal behavior (i.e., of the terminal zone) defines the terminal relaxation time of the "transient network". Qualitatively, like for entangled bulk polymer melts, this terminal relaxation time increases with increasing molecular weight. However, for an end-tethered system one can expect additional restraints which will be evidenced and discussed in sections 3.2 and 4, respectively.

3.1.2. Effect of the Tethering Density. The effect of tethering density is illustrated in Figure 5A,B in the case of the sample PI46K. The 2D viscoelastic properties are shown for two mean areas per molecule, which correspond to the high and low tethering density regime. Figure 5A shows that the general shape of the 2D storage and loss moduli remains unaffected. Two main effects occur upon increasing the tethering density: (i) an increase of the level of both 2D moduli; (ii) a shift of the "terminal zone" to lower frequency, indicating that the terminal relaxation time increases with tethering density.

Figure 5B shows the corresponding frequency dependence of the modulus of the 2D complex viscosity: $|\eta^*(\omega)| = |G'(\omega) + iG''(\omega)|/\omega$. In the terminal zone, it reaches a constant value which is equal to the zero shear viscosity 2D $\eta_0 \equiv \lim_{\omega \to 0} G''(\omega)/\omega$ of the monolayer. One can see that the 2D zero shear viscosity increases with tethering density.

These effects are observed for all molecular weights showing a transient network behavior. We could verify, on the PI-36K sample, that they are reversible upon

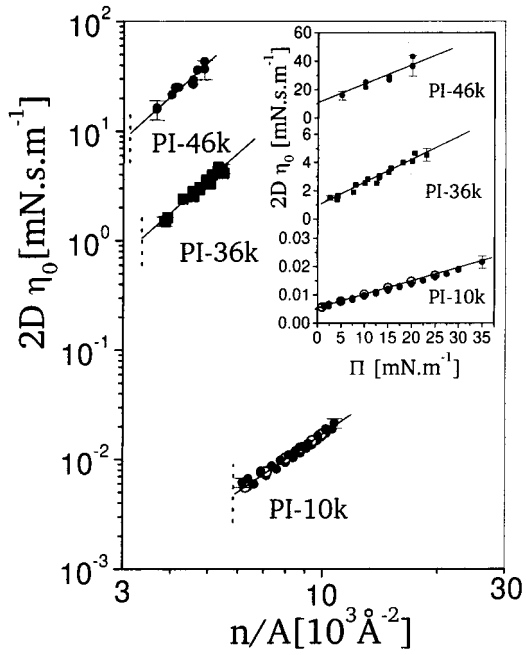

Figure 6. Variation of the 2D zero shear viscosity—in double-logarithmic scale—with the tethering density for the PI-46K, -36K, and -10K samples. For the PI-46K and PI-36K, the zero shear viscosity values have been obtained from the limiting value of the complex viscosity moduli at low frequency. For the sample PI-10K, the viscosities have been determined at a fixed frequency of 3 Hz during compression (filled symbols) and subsequent expansion (open symbols) of the monolayer. The dotted lines mark the lowest possible tethering densities for the molten brushes. The inset shows the same data as a function of the lateral pressure Π. The full lines are drawn as a guide for the eyes.

compression/expansion of the monolayer. Changes of 2D η_0 upon varying the tethering density are shown more in details for the PI-46K as well as for the PI-36K and 10K samples in Figure 6. In the inset one can notice that within the available tethering density range 2D η_0 increases linearly with the lateral pressure. This linear dependence appears to be fulfilled regardless of whether the material exhibits a liquidlike (PI-10K) or a transient network (PI-36K, PI-46K) behavior.

3.2. Effective 3D Viscoelastic Properties of the Brushes and Comparison with the Bulk Properties. In the following, we present the effective 3D properties of the monolayers. The qualitative features of the viscoelastic behavior already discussed for the 2D moduli will not be affected. But this will allow us (i) to determine whether the increase of film thickness upon increasing the tethering density can account for the observed increase of the 2D moduli and viscosity and (ii) to compare directly the properties of the monolayers and bulk polyisoprene melts.

3.2.1. Effective 3D Dynamic Moduli. The frequency dependencies of the effective 3D storage and loss moduli, recalculated from the 2D moduli and the film thicknesses, are plotted in parts A and B of Figure 7, respectively, for the three highest molecular weights (PI-36K, -46K, and -55K) at a constant lateral pressure of $\Pi = 20$ mN/m. To mark the effect of tethering density, we included for the PI-46K the data measured at $\Pi =$ 5 mN/m. Figure 7C shows the corresponding variations of the modulus of the effective 3D complex viscosities.

Notable in Figure 7A,B is that, in the high-frequencies region, the levels of the effective 3D moduli are similar for all molecular weights and tethering densities. Major

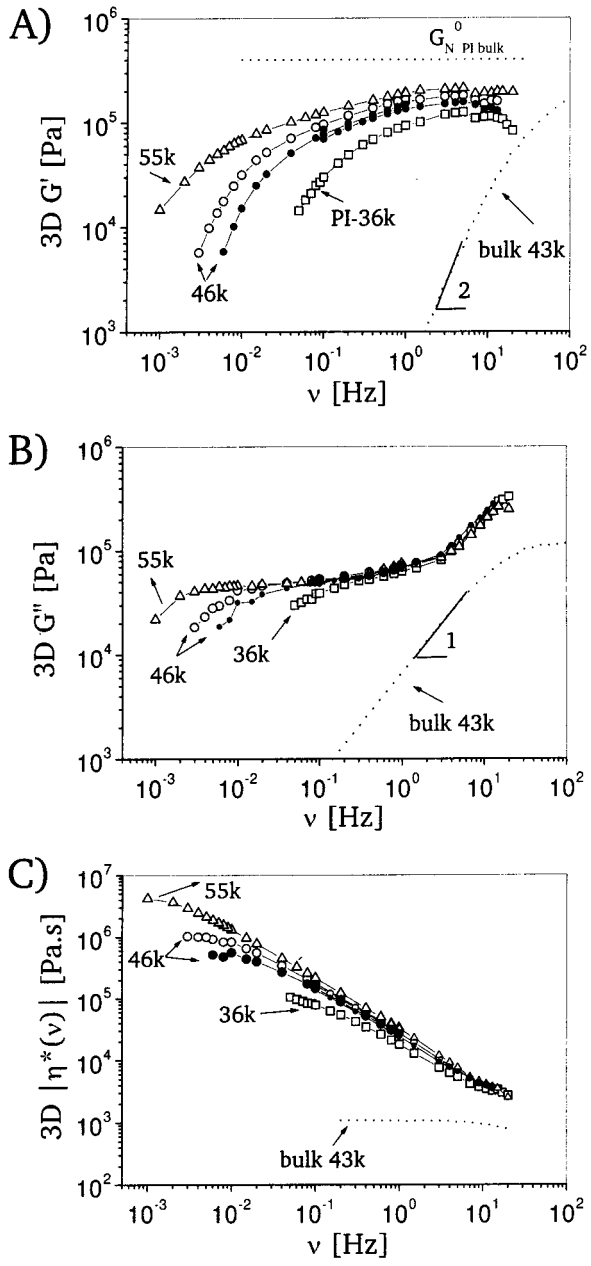

Figure 7. Effective 3D moduli vs frequency on double-logarithmic scales of the samples PI-55K (△), PI-46K (○), and PI-36K (□) at a lateral pressure of $\Pi = 20$ mN/m; for the PI-46K, data at $\Pi = 5$ mN/m (●) are included to illustrate the dependence with surface density; the dotted lines (· · ·) represent data of a linear bulk polyisoprene melt of $M \simeq 43$ kg/mol at $T = 30$ °C taken from ref 30. (A) Storage moduli of the monolayers. The horizontal line (···) marks the level of the plateau modulus of bulk polyisoprene melts, e.g., 4×10^5 Pa. (B) Loss moduli. (C) Modulus of the effective 3D complex viscosities.

differences appear at low frequencies, due to the shift in the onsets of terminal behavior already evidenced with the 2D moduli. At this stage, two main quantities that characterize the transient network are important to compare with the bulk values, the plateau modulus G_N^0 and the terminal relaxation time. For the monolayers, G_N^0 values cannot be determined rigorously as the storage moduli increase continuously in the "plateau region". However, an estimate can be obtained from the level reached by the storage modulus at high frequencies. A close inspection of the curves of Figure 7A suggests that this level increases slightly with molecular

Table 2. Estimated Values of Frequency Onsets for Terminal Behavior and the Corresponding Terminal Relaxation Times: ν_R^{br}, τ_R^{br} for Polyisoprene Brushes at a Lateral Pressure Π; ν_R^{bulk}, τ_R^{bulk} for Linear Bulk Polyisoprenes of Equal Molecular Weight

sample	Π [mN/m]	ν_R^{br} [a] [Hz]	ν_R^{bulk} [a,b] [Hz]	τ_R^{br} [a] [s]	τ_R^{bulk} [a,b] [s]
PI-36K	20	8×10^{-2}	38	80	0.16
PI-46K	20	10^{-2}	16	630	0.4
PI-46K	5	2×10^{-2}	16	315	0.4
PI-55K	20	10^{-3} [c]	8	6300[c]	0.8

[a] ν_R is obtained from the intercept of the lines of slope 1 and 2 describing the dynamic moduli in the terminal zone in a double-logarithmic plot. $\tau_R = 2\pi/\nu_R$. [b] Estimated from the dynamic shear moduli data of refs 28 and 30 assuming $\tau_R \propto M_w^{3.7}$. [c] Extrapolated value.

weight and tethering density while the G'' curves (Figure 7B) appear to coincide perfectly. However, the corresponding variations remain comparable to the deviations of about 20% obtained on different samples measured under the same conditions. Therefore, this effect cannot be addressed quantitatively and should be considered with caution. Nevertheless, for all molecular weights, the values lie in the range $(1-2) \times 10^5$ Pa. Bulk polyisoprene melts exhibit a plateau modulus of about 4×10^5 Pa.[28,29] Hence, the high-frequency level of the storage moduli for the brushlike monolayers is lower but of comparable order of magnitude than in the bulk case.

To compare the terminal relaxation times, we include, in Figure 7A−C, data from ref 30 obtained on a linear bulk polyisoprene melt ($M_w \simeq 43$ kg/mol, polydispersity index $I = 1.13$) with a molecular weight similar to that of our PI-46K sample. One can see that within our experimental frequency range the linear bulk sample exhibits a terminal behavior. It has a terminal relaxation time much shorter than the monolayer. In Table 2, we report the frequency onsets for terminal behavior of the monolayers evaluated from the data of Figure 7A,B. The values and the corresponding relaxation times are compared to those estimated for linear bulk systems. It shows that the terminal relaxation times of end-tethered polymer monolayers are systematically 2−3 orders of magnitude higher and exhibit, at a constant lateral pressure, a much stronger increase with molecular weight.

The moduli of the 3D complex shear viscosities (Figure 7C) show the consequences on the 3D zero shear viscosity which we will now examine in more details: (i) the effective 3D viscosity of the monolayers increases with tethering density; (ii) it increases strongly with molecular weight.

3.2.2. Effective 3D Zero Shear Viscosity: Variation with Tethering Density and Molecular Weight. The variation of 3D η_0 with tethering density is presented in Figure 8 for all molecular weights. In all cases, 3D η_0 increases with tethering density, showing that the observed increase in 2D η_0 not only is due to an increase of film thickness but also reflects an actual increase of the bulk viscosity of the monolayer. The data appear as straight lines in a double-logarithmic as well as in a semilogarithmic plot (inset). Thus, within the accessible tethering density range, the dependence can be described as well with a power law—$\eta_0 \propto (n/A)^\alpha$—as with an exponential—$\eta_0 \propto \exp(\beta n/A)$—increase with tethering density. Assuming a power law, the exponent α is close to 2 for all molecular weights except for the PI-10K sample for which $\alpha \approx 1.5$. This emphasizes that a general dependency appears to be fulfilled for all molecular weights. However, the accessible range of tethering densities is too small to conclude about its specific form.

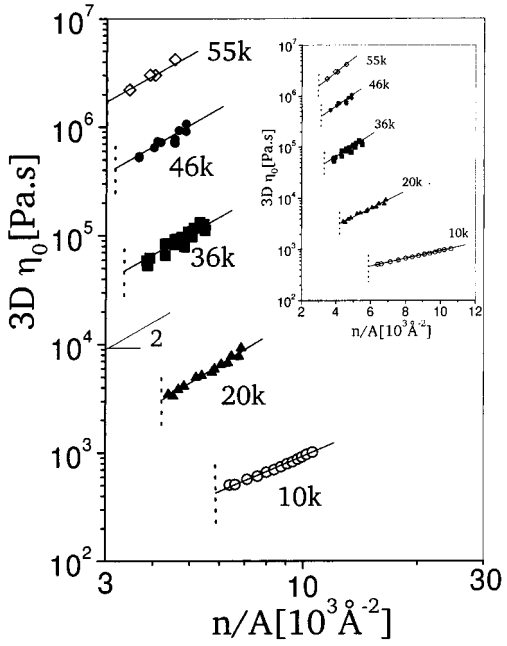

Figure 8. Variation of the effective 3D zero shear viscosity of the brushlike monolayers—in double-logarithmic scale—with the tethering density for the different molecular weights: PI-10K (○), PI-20K (▲), PI-36K (■), PI-46K (●), and PI-55K (◇). The inset shows the same data on a logarithmic−linear scale. The dotted lines indicate, for each molecular weight, the lowest possible tethering density for the molten brush which corresponds with the onset of the isotherm. The full lines are included only as a guide for the eyes.

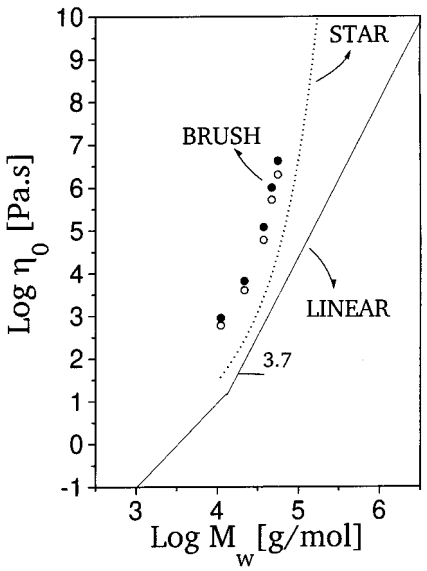

Figure 9. Variation of the zero shear viscosity with the weight-average molecular weight M_w in double-logarithmic scales. Symbols indicate the monolayers data at a constant lateral pressure Π = 5 mN/m (○) and Π = 20 mN/m (●). Lines represent the variations for linear (—) and star (· · ·) polyisoprene melts, deduced from refs 28, 29, 42 and ref 20, respectively. For the stars, arm weight-average molecular weights are used as M_w.

Figure 9 shows in a double-logarithmic plot the brushlike monolayer viscosities as a function of molecular weight. Data are reported at constant lateral

pressure values of 5 and 20 mN/m which represent the low and high surface density regime, respectively. The variations are compared to that observed for linear and star[20] bulk polyisoprenes. As the relaxation times (see Table 2), the zero shear viscosities are orders of magnitude higher than those of the linear bulk systems. More importantly, regardless of the tethering density, the dependence of the monolayers zero shear viscosity with the molecular weight appears to be closer to the exponential form exhibited by the end-tethered bulk system than to the power law dependence[3]—$\eta_0 \propto M^{3-3.7}$—fulfilled by linear melts. Consequences on the relevant type of relaxation mechanisms are examined in the following discussion.

4. Discussion

Our experimental results have shown that the dynamic rheological properties of monolayers of end-tethered chains present a remarkable feature common with that of entangled polymer melts: in a domain of frequency, they behave qualitatively like a rubber. This response is obtained for a shear flow within the interface plane. It marks, undoubtedly, the existence of constraints that inhibit lateral motions. Since the tethered ends can in principle move freely within the interface plane, these constraints are "interchain" in nature, i.e., stem from topological restrictions due to chain uncrossability. In that sense, they are strictly equivalent to the physical entanglements evoked for "free" polymer chains in the bulk.

At this stage, one could argue whether neighboring chains really interpenetrate, according to the traditional picture for free chains in the bulk, or if restriction of lateral motion of individual chain results only from a "caging effect"[11,31] exerted by the (nonpenetrating) neighboring chains.

For a pure caging effect we would expect the relaxation rate of these lateral constraints, i.e., the terminal relaxation time, to depend as much on the surface density as on the molecular weight. Our results clearly show a stronger influence of the molecular weight. A pure caging effect appears therefore not relevant for the constraints probed by the rheological properties, and interpenetration should play a major role.

We will discuss now (i) the degree of interpenetration and (ii) possible relaxation mechanisms in a single layer of (entangled) end-tethered chains.

(i) As we pointed out in the Introduction, it is an important issue to know whether and to which extent the stretching of chains, resulting from end confinement, decreases the onset and the degree of entanglement coupling compared to the bulk case. It seems quite obvious that in the limit of infinitely stretched chains no interpenetration should remain. In a recent computer simulation study on diblock copolymers in the lamellar phase, Murat et al.[31] reported a decrease. Their main arguments were based on the observation of a slight reduction of the number of distinct chain contacts within a lamella compared to the bulk case and that the overall motion of a chain parallel to the interface exceeds the homopolymer tube diameter. In contradiction, simulations by Pan et al.[32] indicated that lamellar ordering does not affect the critical chain length for the onset of entanglement. From our experiments, we get the following insights. Network-like responses appear clearly for a molecular weight of 36 kg/mol, which is approximately 3 times the critical molecular weight $M_{c,bulk}$ of entanglement onset of bulk polyisoprene. Within various models,[3,24] the plateau modulus can be directly related to the entanglement density. In section 3.1.2, we estimated the plateau modulus values for the monolayers from the high-frequency levels of the 3D storage moduli. The values are comparable to the plateau modulus of bulk polyisoprene and do not decrease with increasing tethering density. This indicates that the degree of entanglement does not decrease with tethering density and remain comparable to that in the bulk. So our experiments support that the critical molecular weight as well as the degree of entanglement in a single layer of end-tethered chains are not significantly different than those in the bulk, at least in the experimentally probed range of tethering densities and chain lengths. In this regime, chains remain weakly stretched (see Table 3) as in most practical situations encountered in the melt (e.g., for diblock copolymers). Similarities of both the critical molecular weight and plateau modulus provide further support for a similar nature of topological constraints in the bulk and in monolayers of end-tethered chains.

Table 3. Unperturbed Radius of Gyration $\langle R_G^2\rangle^{1/2}$ [18] and Mean Distances between Chains d_{max}, d_{min} Evaluated from the Mean Area Per Molecules at $\Pi = 1$ mN/m and $\Pi = 30$ mN/m, Respectively; H_{max} and H_{min} Are the Corresponding Heights of the Brush

sample	$\langle R_G^2\rangle^{1/2}$ [Å]	d_{max} [Å]	d_{min} [Å]	H_{min} [Å]	H_{max} [Å]
PI-10K	30	14.7	11.0	103	189
PI-20K	45	17.3	12.8	161	293
PI-36K	60	19.4	14.4	225	411
PI-46K	67	20	15	265	475
PI-55K	73.4	20.8	15.5	295	527

(ii) Concerning the relaxation processes, we have shown that the release of the topological constraints is drastically slowed down for a monolayer of end-tethered chains compared to that for free chains in the bulk. Because of end confinement, disentanglement and thus stress relaxation cannot proceed by conventional reptation motion. As proposed previously in the literature,[8,33−37] an alternative relaxation mechanism is that, like for stars, stress relaxes instead by "arm retraction".[3,27,38] Experimentally, the relevance of this concept has been already shown for the diffusion in diblock copolymers in the lamellar phase,[5,6] systems similar to ours. As the tethered ends are not fixed, one could also consider a disentanglement process by 2D motion of the tethered ends within the interface. Such a mechanism has been described by Rubinstein et al.[36,39] Their analysis suggests that its time scale is longer than the full retraction time and hence that disentanglement by 2D motion may not be a dominant relaxation process.

To discuss the relevance of arm retraction for our systems, we briefly recall some of its implications.[38,40] Arm retraction, entropically unlikely, is thermally activated and leads to an exponential increase of the terminal relaxation time and the zero shear viscosity with the number of entanglements per arm, i.e., with the arm molecular weight. Since entanglements located at different locations from the arm tip relax at different rates, theories based on this process predict a broader relaxation spectrum than for entangled linear chains. These three characteristics are the major differences observed experimentally between star and linear polymer melts.[20,38] For the monolayers, our experiments have shown that both the relaxation times and the zero

shear viscosities appear to increase exponentially with molecular weight (see Table 2 and Figure 9). Though it might be related to the rather short chain lengths of our systems, the frequency dependence of the dynamic moduli reflects a broad relaxation spectrum. In this respect, disentanglement by arm retraction appears to be a relevant mechanism for our systems.

However, it remains an open question why the release of entanglement constraints is slowed down upon increasing surface density. This effect is evidenced by the systematic increase of the terminal relaxation times and zero shear viscosities with tethering density (see Figure 8). For stars, the viscosity has been shown to be independent of the number of arms f when $f \geq 4$.[20] Furthermore, current theories for planar brushes based on arm retraction[34] do not take explicitly into account an effect of tethering density.

An influence of the mean area per molecule could be explained by an increase of the degree of interpenetration. In the frame of a disentanglement process by arm retraction, a slight increase of interpenetration may lead to a significant increase in the relaxation time. Alternatively, the slowing down of the relaxation processes may result only from the increased anisotropy of the system. We hope that our experimental observations will stimulate specific theoretical developments addressing this point.

Finally, we would like to emphasize some general implications for layers of end-tethered chains. Our results indicate that chains within a polymer brush can be entangled like in the bulk case. This should hold for chains end-grafted to a liquid as well as to a solid substrate. For liquid interfaces, it implies that unusually slow relaxations can occur. Such slow relaxation has been evidenced recently for polymer blends compatibilized by diblock copolymers.[41] The rheological properties of these bulk systems reveal a new relaxation process which has been attributed to a finite shear modulus of the interface. The corresponding time scales, 2−3 orders of magnitude larger than those associated with the relaxation of the blend components, are indeed comparable to the times scales evidenced in our experiments.

5. Conclusions

We presented a new experimental approach that provides the following insight into the dynamics of a single layer of end-tethered chains. Like free chains in the bulk, long chains in an end-tethered polymer monolayer develop entanglement-like topological constraints. Their release is by orders of magnitude slower than for a melt of free chains. The terminal relaxation time and the zero shear viscosity have been shown (i) to exhibit an enhanced molecular weight dependence and (ii) to increase upon increasing the tethering density. The first aspect can be qualitatively understood by a disentanglement process, as for star polymers, via arm retraction. The second provides, to our knowledge, the first experimental evidence for a slowing down of relaxation processes upon increasing tethering density. Whether it reflects a slight increase in the degree of interpenetration or only an effect of anisotropy on relaxation processes remains an open question. Further theoretical developments would be required in order to settle whether arm retraction can provide a molecular picture coherent with both experimental observations.

Acknowledgment. We thank R. Heger, who synthesized the polymers used in this study and determined their thermodynamic properties, as well as J. Krägel for preliminary measurements on his interfacial rheometer. The support and fruitful comments of Prof. Antonietti and Prof. Möhwald are gratefully acknowledged. C.L. also thanks F. Lequeux and M. Rubinstein for helpful discussions as well as the Max-Planck Society for financial support through a Schloessmann fellowship.

References and Notes

(1) de Gennes, P. G. *Macromolecules* **1980**, *13*, 1069−1075.
(2) Milner, S. T. *Science* **1991**, *251*, 905−914.
(3) Doi, M.; Edwards, S. F. *The Theory of Polymer Dynamics;* Clarendon Press: Oxford, 1986.
(4) Yao, M.-L.; Watanabe, H.; Adachi, K.; Kotaka, T. *Macromolecules* **1991**, *24*, 2955−2962.
(5) Lodge, T. P.; Dalvi, M. W. *Phys. Rev. Lett.* **1995**, *75*, 657−660.
(6) Lodge, T. P.; Hamersky, M. W.; Milhaupt, J. M.; Kannan, R. M.; Dalvi, M. C.; Eastman, C. E. *Macromol. Symp.* **1997**, *121*, 219−233.
(7) Fytas, G.; Anastasiadis, S. H.; Seghroughni, R.; Vlassopoulos, D.; Li, J.; Factor, B. J.; Theobald, W.; Toprakcioglu, C. *Science* **1996**, *274*, 2041−2044.
(8) Klushin, L. I.; Skvortsov, A. M. *Macromolecules* **1991**, *24*, 1549−1553.
(9) Koch, M.; Sommer, J. U.; Blumen, A. *J. Chem. Phys.* **1997**, *106*, 1248−1256.
(10) Murat, M.; Grest, G. S. *Macromolecules* **1989**, *22*, 4054−4059.
(11) Milik, M.; Kolinski, A.; Skolnick, J. *J. Chem. Phys.* **1990**, *93*, 4441−4446.
(12) Lai, P. Y.; Binder, K. *J. Chem. Phys.* **1992**, *97*, 586−595.
(13) Klein, J. *Annu. Rev. Mater. Sci.* **1996**, *26*, 581−612.
(14) Hu, H.-W.; Granick, S. *Science* **1992**, *258*, 1339−1342. Hu, H.-W.; Granick, S. *Langmuir* **1994**, *10*, 3857−3866.
(15) Dhinojwala, A.; Cai, L.; Granick, S. *Langmuir* **1996**, *12*, 4537−4542.
(16) Pelletier, E.; Belder, G. F.; Hadziioannou, G.; Subbotin, A. *J. Phys. II* **1997**, *7*, 271−283.
(17) The lateral pressure Π is the difference between the surface tensions of the bare water surface and the film-covered water surface.
(18) Heger, R.; Goedel, W. A. *Macromolecules* **1996**, *29*, 8912−8921.
(19) Odani, H.; Nemoto, N.; Kurata, M. *Macromolecules* **1972**, *5*, 531−535.
(20) Fetters, L. J.; Kiss, A. D.; Pearson, D. S.; Quack, G. F.; Vitus, F. G. *Macromolecules* **1993**, *26*, 647−654.
(21) Baltes, H.; Schwendler, M.; Helm, C. A.; Heger, R.; Goedel, W. A. *Macromolecules* **1997**, *30*, 6633−6639.
(22) Krägel, J.; Li, J. B.; Miller, R.; Bree, M.; Kretzschmar, G.; Möhwald, H. *Colloid. Polym. Sci.* **1996**, *274*, 1183−1187.
(23) Warburton, B. In *Rheological Measurements*, 2nd ed.; Collyer, A. A., Clegg, D. W., Eds.; Chapman & Hall: London, 1998; pp 723−754.
(24) Ferry, J. D. *Viscoelastic Properties of Polymers*, 3rd ed.; Wiley & Sons: New York, 1980.
(25) Sherriff, M.; Warburton, B. In *Theoretical Rheology*; Holten, J., Pearson, J., Walters, K., Eds.; Applied Science: London, 1975; pp 299−316.
(26) For most of the polymers (PI-36K and higher molecular weights), the (viscous) contribution due to pure water subphase is negligible compared with that due to the monolayer. For the lowest molecular weight, both contributions are of the same order of magnitude.
(27) de Gennes, P. G. *Scaling Concepts in Polymer Physics*, 4th ed.; Cornell University Press: Ithaca, NY, 1993.
(28) Gotro, J. T.; Graessley, W. W. *Macromolecules* **1984**, *17*, 2767−2775.
(29) Pearson, D. S.; Mueller, S. J.; Fetters, L. J.; Hadjichristidis, N. *J. Polym. Sci., Polym. Phys. Ed.* **1983**, *21*, 2287−2298.
(30) Fodor, J. S.; Huljak, J. R.; Hill, D. A. *J. Chem. Phys.* **1995**, *103*, 5725−5734.
(31) Murat, M.; Grest, G. S.; Kremer, K. *Europhys. Lett.* **1998**, *42*, 401−406.
(32) Pan, X. H.; Shaffer, J. S. *Macromolecules* **1996**, *29*, 4453−4455.

(33) Witten, T. A.; Leibler, L.; Pincus, P. A. *Macromolecules* **1990**, *23*, 824−829.
(34) Joanny, J. F. *Langmuir* **1992**, *8*, 989−995.
(35) Nemirovsky, A. M.; Witten, T. A. In *Complex Fluids;* Springer-Verlag: Heidelberg, 1993; pp 281−293.
(36) Rubinstein, M.; Obukhov, S. P. *Macromolecules* **1993**, *26*, 1740−1750.
(37) Klein, J.; Kumacheva, E.; Perahia, D.; Fetters, L. J. *Acta Polym.* **1998**, *49*, 617−625.
(38) Pearson, D. S.; Helfand, E. *Macromolecules* **1984**, *17*, 888−895.
(39) Obukhov, S. P.; Rubinstein, M. *Phys. Rev. Lett.* **1990**, *65*, 1279−1282.
(40) Milner, S. T.; McLeish, T. C. B. *Macromolecules* **1997**, *30*, 2159−2166.
(41) Riemann, R. E.; Cantow, H. J.; Friedrich, C. *Macromolecules* **1997**, *30*, 5476−5484.
(42) Georges, J. M.; Millot, S.; Loubet, J. L.; Tonck, A. *J. Chem. Phys.* **1993**, *98*, 7345−7360.

MA991485I